

M. HEBDA\*, S. GADEK\*, J. KAZIOR\*

## INFLUENCE OF THE MECHANICAL ALLOYING PROCESS ON THE SINTERING BEHAVIOUR OF ASTALOY CrM POWDER MIXTURE WITH SILICON CARBIDE ADDITION

### WPLYW PROCESU STOPOWANIA MECHANICZNEGO NA ZJAWISKA ZACHODZĄCE PODCZAS SPIEKANIA PROSZKU ASTALOY CrM MODYFIKOWANEGO DODATKIEM WĘGLIKA KRZEMU

Due to an excellent combination of toughness and strength, bainitic-austenitic dual phase steels with silicon addition have many applications in the industry. However, silicon has a high affinity to oxygen and, therefore, its introduction to the alloy is problematic during the classical sintering processes of mixing powders. Mechanical alloying (MA) offers one of the most attractive alternatives to the introduction of silicon to Astaloy CrM powders.

The aim of the present study was to determine the influence of the MA process on changes in particle size distribution, work hardening and sintering behaviour of the investigated powder mixture – Astaloy CrM powder with the addition of 2 wt.% stearic acid and 2 wt.% silicon carbide alloyed under different conditions. The practical aspect of this study was to develop and apply a common and inexpensive method of die-pressing to compact a powder mixture prepared by the MA process.

*Keywords:* mechanical alloying, Astaloy CrM, silicon carbide, dilatometric analysis, mass spectrometry analysis

Dwufazowe stale bainityczno-austenityczne ze względu na swoje właściwości wytrzymałościowe i plastyczne mają coraz szersze zastosowanie w przemyśle. Jednakże wprowadzanie do składu mieszanek dodatku krzemu nastęca wiele problemów technologicznych podczas klasycznego spiekania materiałów proszkowych m.in. poprzez duże powinowactwo tego pierwiastku do tlenu. Proces mechanicznego stopowania oferuje jedno z alternatywnych rozwiązań wprowadzenia krzemu do niskostopowych proszków Astaloy CrM.

W pracy przedstawiono wyniki badań wpływu procesu mechanicznego stopowania na zmiany wielkości cząstek proszku, ich utwardzenie oraz efekty zachodzące podczas spiekania mieszanek: Astaloy CrM z dodatkiem 2% wg kwasu stearynowego i 2% wg węgliku krzemu, wytworzonych w różnych warunkach stopowania. Praktycznym aspektem przeprowadzonych badań było uzyskanie mieszanek po procesie stopowania mechanicznego nadających się do formowania matrycowego, jako najtańszej i najbardziej rozpowszechnionej metody kształtowania wyrobów proszkowych.

## 1. Introduction

Since the pioneering work of Benjamin [1], which was concentrated on the production of nickel superalloys hardened by oxide dispersion, considerable effort has been put into extending the range of materials and alloys that can effectively be processed by mechanical alloying/milling (MA). Nowadays MA, as a non-equilibrium processing technique, is extensively used for the preparation of supersaturated solid solutions, amorphous materials, intermetallic compounds and metal matrix composites [2, 3]. The MA process consists of the repeated welding-fracturing-welding of a mixture of powder particles in a high-energy ball mill. The powder particles are trapped between the colliding balls during milling and

undergo deformation, welding or fracture, depending on the mechanical behaviour of the powder components, so that powder particles with a very fine structure can be obtained after MA [2].

The main advantage of MA is that reactions which normally occur at high temperatures may take place at low temperatures. The restriction imposed by the thermodynamic phase diagram is overcome by mechanical alloying. This is evident in the formation of meta-stable phases and a supersaturated solid solution.

The disadvantages or limitations of powders prepared by the MA method are surface hardening and decrease in particle size. These factors discriminate the classical method of compaction, therefore, Hot Isostatic Pressing (HIP), Selective Laser Sintering (SLS), Pow-

\* CRACOV UNIVERSITY OF TECHNOLOGY, FACULTY OF MECHANICAL ENGINEERING, 31-155 KRAKÓW, 24 WARSZAWSKA STR., POLAND

der Injection Moulding (PIM) or Spark Plasma Sintering (SPS) are more efficient for powder compaction after the MA process.

We chose MA as the most useful process to obtain a combination of low-alloy steel with silicon addition. Such a mixture should improve toughness and strength of bainitic-austenitic dual phase steels and can be applicable in many branches of the industry [4, 5].

The aim of this work was to study the influence of the mechanical alloying process of Astaloy CrM powder with silicon carbide addition on changes in particle size distributions, work hardening and sintering behaviour of the investigated powder mixture. Also investigated were the influences of some process parameters, e.g. powder to ball mass ratio and milling times/number of alloying cycles on the material properties. The practical aspect of our study was the development and application of an inexpensive method of die-pressing to compact a powder mixture prepared by the MA process.

## 2. Experimental procedure

### Material

The specimens were prepared by mechanical alloying of Astaloy CrM powders (water atomised iron powder with the chemical compositions of 3.0 wt.% Cr and 0.5 wt.% Mo manufactured and supplied by Höganäs) with 2 wt.% stearic acid (supplied by Sigma-Aldrich) and 2 wt.% silicon carbide (supplied by Sigma-Aldrich).

Stearic acid ( $\text{CH}_3(\text{CH}_2)_{16}\text{COOH}$ ) was added to the powder mixture as the agent (process control agent – PCA) with the aim of controlling the mechanical alloying process and, in principle, to avoid powder particle agglomeration.

### Methods

#### Mechanical Alloying

For MA, a highly energetic planetary mono-ball mill (Fritsch, Pulverisette 6 model) was used. The process was carried out in a tempered steel container equipped with grinding balls 10 mm in diameter, in a vacuum atmosphere. The powder to ball mass ratio was 2:1, 1:1, and 1:10. The milling time was 3 min, intermission period was 30 min, rotary speed 500 [rot/min], and the number of cycles was 20, 40 and 200.

#### Compactibility

The Astaloy CrM powder and powders after the MA process were uni-axially compacted under pressures of 300, 400, 500 and 600 MPa in the form of discs 20 mm in diameter and 5 mm in height.

#### Dilatometric studies

Sintering behaviour was performed in a horizontal NETZSCH 402 C dilatometer. The powders were uni-axially compacted at 600 MPa, giving cylindrical green compacts 5 mm in diameter and 10 mm in length, respectively. The process was performed in high purity (6.0) hydrogen or a mixture atmosphere of helium with 10 wt.% hydrogen, under 100 ml/min flowing atmosphere. The heating and cooling rates were 10°C/minute. The isothermal sintering temperature was 1150°C. The holding time at the isothermal sintering temperature was 30 min. Two replicates were measured. Data were analysed with the use of Proteus software (ver. 5.2.0) supplied by Netzsch.

#### Thermogravimetric/Quadruple Mass Spectrometry studies

Thermal measurements were performed with STA 409 CD (Netzsch) advanced coupling techniques including evolved gas analysis by Quadruple Mass Spectrometry (QMS 403/5 SKIMMER). The thermogravimetric analysis was performed using a closed aluminium crucible (85  $\mu\text{l}$ ), with a 50  $\mu\text{m}$  hole in the lead. Crucibles were filled with about 150 mg of the samples. Data were recorded under a dynamic flow (80 ml/min) of helium or helium with 10 wt.% hydrogen atmosphere (purity 5.0). The heating temperature range was from 30°C to 1150°C and the heating/cooling rate was 10°C/min. The holding time at the isothermal sintering temperature was 30 min.

The on-line gas analysis for all measurements was studied by QMS with an electron ionisation source. The spectrometer was operated in Scan Bargraph mode (from  $m/z$  5 up to  $m/z$  100). The QMS was tested using Calcium Oxalate Monohydrate (Fluka). Two replicates of each experimental sample were measured. The ion current curves of recorded mass (as a Quasi Multiple Ion Detection – QMID) during the whole sintering process were calculated with Proteus software (ver. 5.2.0) supplied by Netzsch.

#### Particle size measurements

Particle size distribution was determined by laser diffraction (Fritsch Analysette 22 MicroTec plus model). Volume size distribution was calculated automatically and expressed as D10, D50 (median) and D90. Five measurements were carried out for each sample.

#### Microhardness

Microhardness HV0.01 (model Nexus 423A with Nexus Inv-1) was performed for the included powders at room temperature and at least ten replicates were measured.

### 3. Results and discussion

The MA process is affected by several factors that play a very important role in the fabrication of materials and properties of the final products. The chief factor controlling the mechanical alloying process are the milling conditions: milling atmosphere (e.g. inert/controlled gas or vacuum), milling environment (e.g. dry milling or wet milling), powder to ball mass ratio, types and sizes of milling media, milling time and type of milled materials [6,7].

For a better understanding of the influence of mechanical alloying on changes in particle size distribution and surface work hardening we used a mixture of Astaloy CrM with 2 wt.% PCA and 2 wt.% SiC. The Astaloy CrM powder with the addition of silicon carbide (reinforcement particles) is a typical example of a ductile/brittle component system (e.g. J.B. Fogagnolo et al. [8] proposed and explained this alloyed model). Our earlier experiment indicated that the powder to ball mass ratio used in experiments should be in the range from 3:1 to 1:50 (data not shown). Generally, it was determined that the time needed for particle fragmentation decreased when the ball mass increased (and other factors were constant). Therefore, we chose powder to ball mass ratio to be 2:1, 1:1, and 1:10. Moreover, a variable parameter was the milling time at 1, 2 and 10 h.

Figure 1 shows the particle size distributions for the Astaloy CrM and MA mixtures obtained under different conditions of milling. The vertical lines refer to the equivalent diameters (D50, median). The majority of grains for the base Astaloy CrM powder had the average

diameter of  $80.00 \pm 1.01 \mu\text{m}$  (Fig. 1A). Particles after 1 h of MA with the powder to ball mass ratio at 1:10 decreased the equivalent diameters ( $D_{50} = 45.90 \pm 4.98 \mu\text{m}$ ), however, the span of peak was much wider comparing to the non-milled powders (Fig. 1B, Tab. 1). The longest milling time (2 h) caused a continuous decrease of particle size ( $D_{50} = 32.97 \pm 1.15 \mu\text{m}$ ) (Fig. 1E). When silicon carbide was added to the powder mixture and milling time was 2 h, the average particle size increased significantly to  $83.48 \pm 2.97 \mu\text{m}$  (Fig. 1H). These results indicated that the presence of silicon in the mixture made the milling process difficult. Welding is the predominant phenomenon for powder mixture with silicon carbide additions, in contrast to plastic deformation characteristic for the milling of the base powder. The biggest particles were recorded after 2 h of the MA process for the 1:1 ratio (Fig. 1G), suggesting that particle shape was flattened and some particles were welded to each other. For the mixture with the silicon addition, the smallest particle size was recorded after 10 h of milling with the 1:10 ratio (Fig. 1I). When the powder to ball mass ratio was 2:1, 10 h of milling gave particles with an average size around  $95.31 \pm 3.23 \mu\text{m}$  (Fig. 1J). It is also worth noting that the results for the 2:1 ratio were dependent on the milling time – the longer milling time progressively increased particle size (Fig. 1C, Fig. 1D, Fig. 1F, Tab. 1). These results showed that the particle did not reach the stage when the brittle behaviour dominated and led to particle fragmentation, therefore we concluded that die compaction for the alloying of Astaloy CrM compositions should be possible under a 2:1 powder to ball mass ratio.

TABLE 1  
Median and span of particle size distributions of Astaloy CrM and MA mixing powders after different conditions of milling

Material	Milling time (h)	Powder to ball mass ratio	D50 ( $\mu\text{m}$ )	Span ( $\mu\text{m}$ ) (D90-D10)/D50
Astaloy CrM base powder	0	–	$80.00 \pm 1.01$	$0.97 \pm 0.07$
Astaloy CrM + 2 wt.% PCA	1	1:10	$45.90 \pm 4.98$	$2.47 \pm 0.12$
	2	1:10	$32.97 \pm 1.15$	$1.52 \pm 0.08$
	2	2:1	$94.39 \pm 3.72$	$1.60 \pm 0.03$
Astaloy CrM + 2 wt.% PCA + 2 wt.% SiC	1	2:1	$62.08 \pm 2.49$	$2.13 \pm 0.04$
	2	2:1	$81.57 \pm 5.04$	$1.99 \pm 0.17$
	2	1:1	$125.95 \pm 5.08$	$1.58 \pm 0.03$
	2	1:10	$83.48 \pm 2.97$	$1.96 \pm 0.07$
	10	1:10	$14.24 \pm 0.21$	$2.15 \pm 0.04$
	10	2:1	$95.31 \pm 3.23$	$1.82 \pm 0.07$

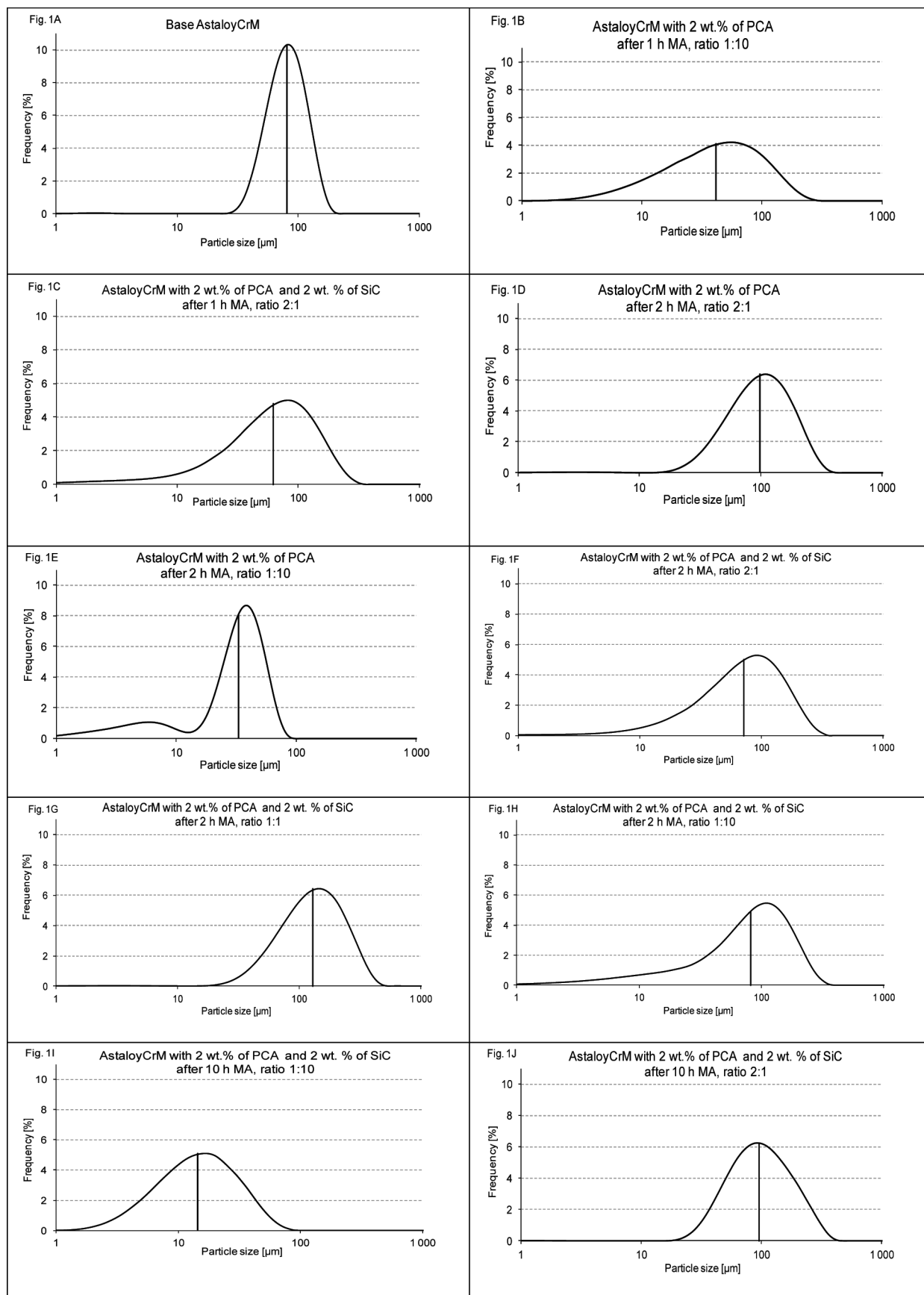


Fig. 1. Particle size distributions for the Astaloy CrM and MA mixtures under different conditions (milling time and powder to ball mass ratio). Vertical lines refer to the D50 diameter

Table 2 presents the results of the microhardness HV0.01 of the investigated samples under different conditions (milling time and powder to ball mass ratio). It was determined that an increase of microhardness of the investigated mixtures corresponded to the cold welding, fracturing and rewelding phenomenon.

The highest value of microhardness was measured for powders achieved in the 1:10 powder to ball mass ratio. Microhardness of the base powder after 2 h of milling was about  $963 \pm 161$  HV0.01. The large value of standard deviation indicated a high heterogeneity of the powder mixture and the lack of balance between cold welding and fracturing. The mixture with silicon carbide, after 10 h of milling, reached a maximum of work hardening ( $1419 \pm 150$  HV0.01) due to cold working of the particles. Therefore, this powder, due to the fragmentation of particles resulting from a drastic increase of

hardness, cannot be die compacted, where plastic deformation is the primary process. In contrast, microhardness of the mixture milled in the 2:1 powder to ball mass ratio was about 165 HV0.01 and the results did not depend on the milling time.

Figure 2 demonstrates the compactibility curves of Astaloy CrM and the mixture after the MA process under different conditions. It is obvious that the compactibility of powders strongly depends on several factors, e.g. particle size, shape and chemical composition. The best compaction within the analysed powder was observed for the base Astaloy CrM. When the compacting pressure increased from 300 MPa to 600 MPa, the density of green elements also increased linearly. After the MA process, only powder milled with the lower powder to ball mass ratio (2:1 and 1:1) was suitable for die compaction. The compactibility of these compositions was

TABLE 2

Microhardness HV0.01 of the investigated samples after different conditions of milling (milling time and powder to ball mass ratio)

Material	Milling time (h)	Powder to ball mass ratio	Microhardness HV0.01
Astaloy CrM base powder	0	–	$78 \pm 14$
Astaloy CrM + 2 wt.% PCA	1	1:10	$74 \pm 16$
	2	1:10	$963 \pm 161$
	2	2:1	$146 \pm 38$
Astaloy CrM + 2 wt.% PCA + 2 wt.% SiC	1	2:1	$136 \pm 25$
	2	2:1	$174 \pm 25$
	2	1:1	$187 \pm 33$
	2	1:10	$158 \pm 40$
	10	1:10	$1419 \pm 150$
	10	2:1	$164 \pm 39$

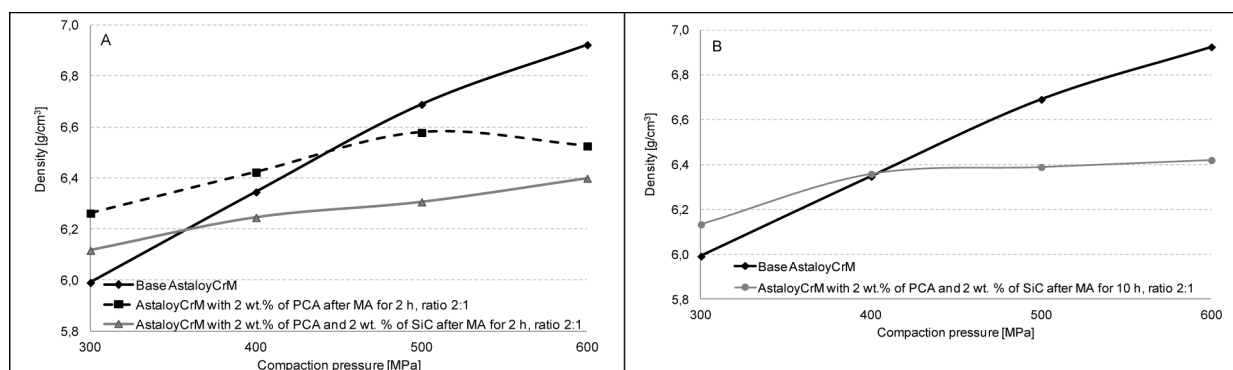


Fig. 2. Relationship between density and pressure during compaction of various Astaloy CrM compositions a) alloyed 2 h, b) alloyed 10 h

less effective than for the base powder, especially for the higher pressure value. This effect was independent on the analysed compositions and likely corresponded to the lack of plastic deformation, hardening, and consequently, particle size fragmentation. Astaloy CrM with 2 wt.% PCA and 2 wt.% SiC after 10 h of milling (2:1 ratio) did not change density when compaction pressure exceeded 400 MPa. On the other hand, all alloyed compositions compacted with pressure of 300 MPa gave better results in comparison to the base Astaloy CrM density. This effect probably originated from particle deformation and welding during the MA process. Powders after MA with a 1:10 powder to ball mass ratio were useless for directed die compactations because of particle hardening, accumulation of large compressive strains during alloying and decrease of particle size.

A thermal dilatometry was employed to compare the sintering process of the MA mixtures and the base Astaloy CrM powder. Representative examples of plots

recorded during the dilatometric analyses are shown in Figures 3–6. The Astaloy CrM powders were sintered in two various atmospheres: pure hydrogen and a mixture of helium with 10 wt.% hydrogen (hydrogen as a reduction agent). During heating to the isothermal sintering temperature, Astaloy CrM showed a continuous thermal expansion with a sharp shrinkage at about 900°C, as a consequence of the  $\alpha\text{Fe} \rightarrow \gamma\text{Fe}$  transformation. During isothermal holding the Astaloy CrM showed a shrinkage (less for the helium/hydrogen atmosphere) which was continued during cooling. Between 900°C – 870°C, the  $\gamma\text{Fe} \rightarrow \alpha\text{Fe}$  transformation was registered. The sintering curve recorded in the mixture of helium and hydrogen was below the curve taken in the hydrogen atmosphere. This was a result of the thermal conductivity of the used gases. The Astaloy CrM with the addition 2 wt.% PCA showed drastic shrinkage during heating, which started at about 665°C as a result of removal/evaporation of the organic agent from the specimen.

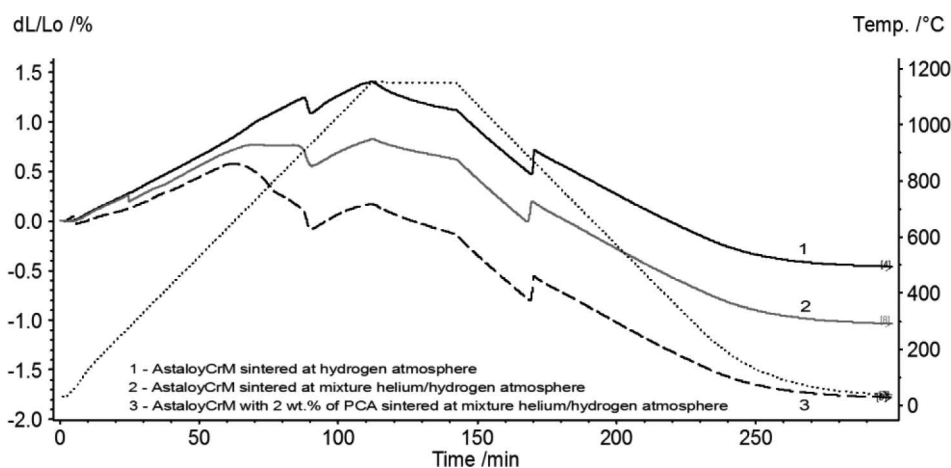


Fig. 3. Dilatometric plots of non-alloyed Astaloy CrM and Astaloy CrM with addition of 2 wt.% PCA sintered in an atmosphere of hydrogen and mixture of helium with 10 wt.% hydrogen

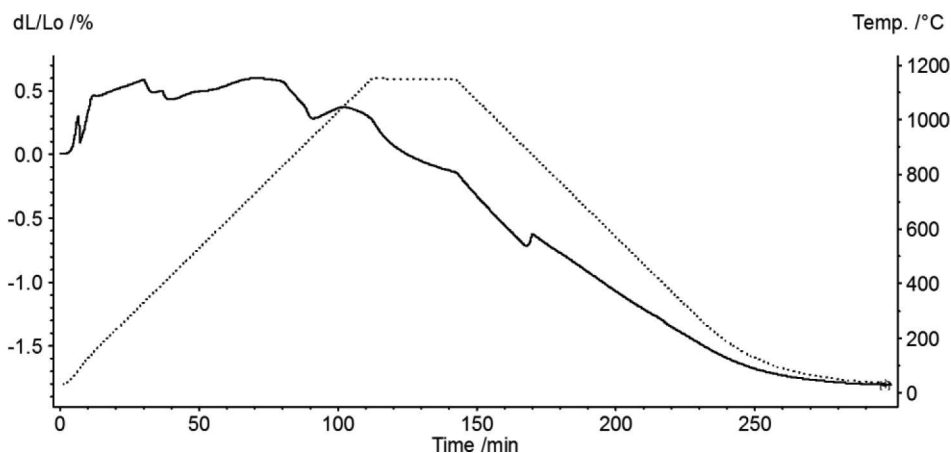


Fig. 4. Dilatometric curve of Astaloy CrM with addition of 2 wt.% PCA (2:1 ratio) after MA for 2 h, sintered in an atmosphere of helium with 10 wt.% hydrogen mixture

The dilatometric curve obtained for Astaloy CrM with the addition of 2 wt.% PCA after 2 h of milling (2:1 ratio) sintered in a helium/hydrogen atmosphere showed significant changes (in comparison to the base powder), mainly during the heating stage (Fig. 4). The swelling of samples was detected from the beginning of heating. This process was finished at about 425°C, which indicated the removal of organic compounds. However, this hypothesis is not confirmed by a similar effect for a non-alloyed composition supplemented with PCA. Hence, we concluded that this effect was dependent on the accumulation of large compressive strains during alloying. Moreover, the MA process shifted the onset of the transformation  $\alpha\text{Fe} \rightarrow \gamma\text{Fe}$  to the lower temperature range. The intensity of peaks registered during heating and cooling was also much smaller.

A similar effect for compositions with silicon carbide sintered in a helium/hydrogen atmosphere was detected during heating (Fig. 5), i.e. the longer the milling time, the higher the swelling. Moreover, the presence of silicon in the samples suppressed lattice transformation during heating and cooling. Exceeding 2 h of milling for the 2:1 ratio started the sintering process before the isothermal step. This effect was initiated simultaneously with the lattice transformation (around 830°C).

Different results were obtained for processes in the pure hydrogen atmosphere. The swelling effect was not as evident during heating. Moreover, the lattice transformation occurring simultaneously with shrinkage appeared much earlier (starting from 1 h of the milling process), in comparison to the processes in the helium/hydrogen atmosphere (Fig. 5 and 6).

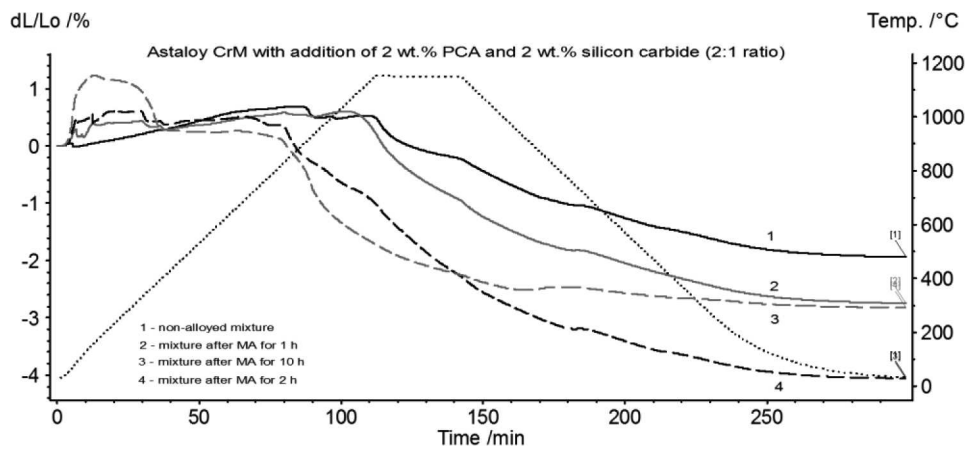


Fig. 5. Dilatometric curves of base Astaloy CrM with addition of 2 wt.% PCA and 2 wt.% silicon carbide (2:1 ratio) after 1 h, 2 h and 10 h of MA, sintered in an atmosphere of helium with 10 wt.% hydrogen mixture

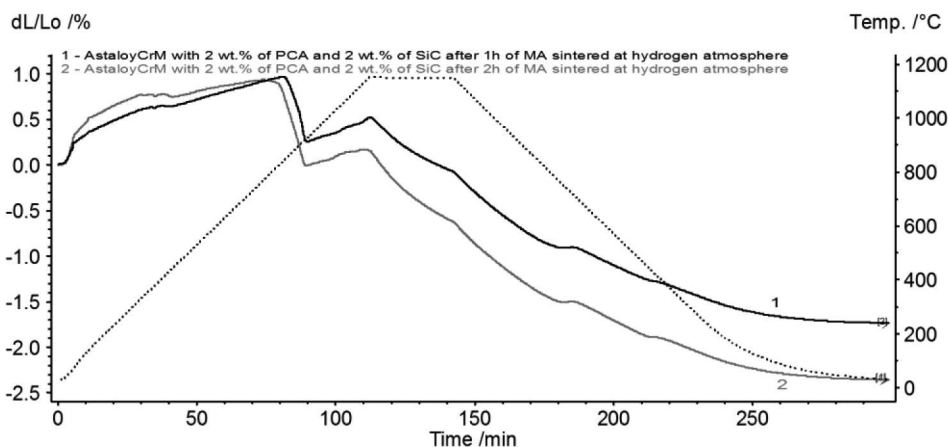


Fig. 6. Dilatometric curves of Astaloy CrM with addition of 2 wt.% PCA and 2 wt.% silicon carbide (2:1 ratio) after 1 h and 2 h of MA, sintered in a pure hydrogen atmosphere

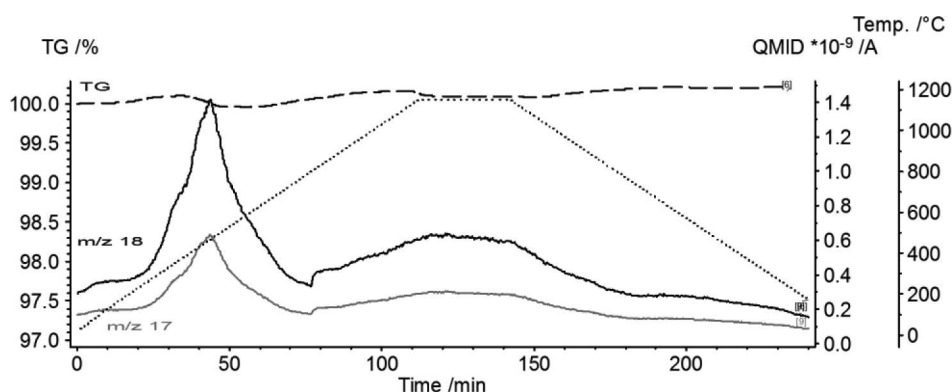


Fig. 7. TG and QMID curves for Astaloy CrM powder sintered in an atmosphere of helium with 10 wt.% hydrogen mixture

Figure 7 shows that 10 wt.% hydrogen in a helium atmosphere was sufficient to initiate the reduction of metallic oxides from the surfaces of the sintered base Astaloy CrM powders. Two inflections corresponding to mass losses were recorded on the TG curve: the first during heating, between 380°C and 490°C, the second during both the isothermal step and cooling to 1000°C. An on-line gas analysis with QMS allowed us to interpret such effects. At temperatures of mass losses a high increase of  $m/z$  18 and 17 was detected. The curves were parallel and an intensity of  $m/z$  17 was about 1/3 lower than  $m/z$  18. Since  $m/z$  18 and  $m/z$  17 corresponded to  $H_2O$  productions resulting from moisture removal, the desorption of physically bonded water and start of the reduction of the surface iron oxides in the high temperature range.

It is a well-known fact that the sintering of iron powder in an inert atmosphere does not induce any ef-

fect on the thermogravimetric curves (Fig. 8). The TG curve of Astaloy CrM with 2 wt.% PCA showed one big mass loss finished at 450°C, which corresponded to the amount of organic compounds (some small differences in mass losses within the analysed compositions could be the results of a heterogeneous mixture).

The mechanical alloying process of Astaloy CrM with 2 wt.% PCA (with the 2:1 ratio) caused the evaporation of PCA much earlier at temperature 100°C higher than the evaporation observed for a non-alloyed composition. Moreover, the decomposition of organics proceeded as a one-step process in comparison to a two-step mass loss for a non-alloyed mixture (Fig. 8 and Fig. 9). Furthermore, for samples with silicon carbide, additional mass losses during isothermal sintering were observed (Figs. 8 and 12). This effect corresponded to the presence of carbon in the samples and to its oxidation (Fig. 12).

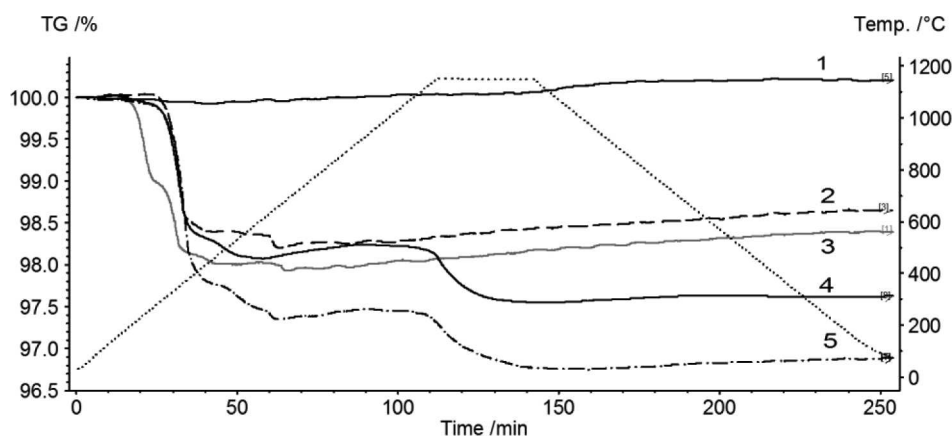


Fig. 8. TG curves of various Astaloy CrM compositions sintered in a helium and helium with 10 wt.% hydrogen atmosphere: 1 – Astaloy CrM sintered in helium, 2 – Astaloy CrM with 2 wt.% PCA, 2h alloyed sintered in helium, 3 – Astaloy CrM with 2 wt.% PCA non-alloyed sintered in helium, 4 – Astaloy CrM with 2 wt.% PCA and 2 wt.% SiC, 2 h alloyed sintered in helium, 5 – Astaloy CrM with 2 wt.% PCA and 2 wt.% SiC, 2 h alloyed sintered in helium/hydrogen atmosphere

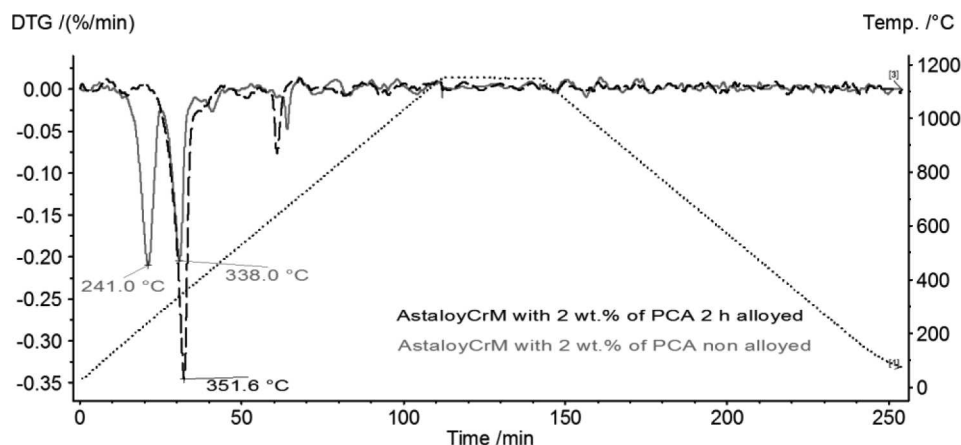


Fig. 9. DTG curves of Astaloy CrM with 2 wt.% PCA, 2 h alloyed and non-alloyed sintered in a helium atmosphere

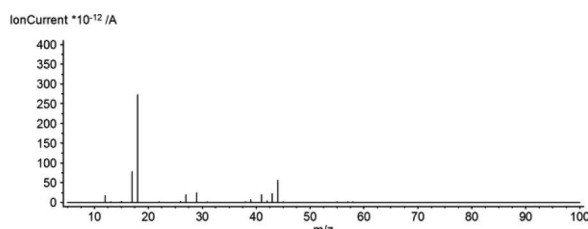


Fig. 10. Bargraph at 350°C of Astaloy CrM with 2 wt.% PCA (non-alloyed) sintered in a helium atmosphere

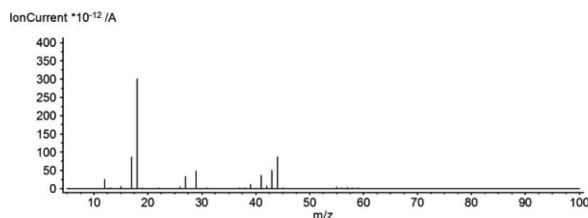


Fig. 11. Bargraph at 350°C of Astaloy CrM with 2 wt.% PCA after MA for 2 h (2:1 ratio) sintered in a helium atmosphere

Figures 10 and 11 present gas bargraph signals of PCA decomposition originating from the Astaloy CrM mixture (alloyed and non-alloyed). These bargraphs were determined at maximum of decomposition kinetic (around 350°C) on DTG curves (Fig. 9). The bargraphs are similar for the alloyed and non-alloyed Astaloy CrM mixture.

Figure 12 shows differences in the intensity of masses between sintering in a helium (inert) and helium/hydrogen atmosphere for Astaloy CrM powder with 2 wt.% PCA and 2 wt.% SiC milled at 2 h in the 2:1 ratio. The protected atmosphere with hydrogen reduced metal oxides more effectively. The masses presented in Figure 12 were the main products of reduction corresponding to water ( $H_2O$  – masses  $m/z$  18,  $m/z$  17,  $m/z$

16) and carbon monoxide ( $CO$  – masses  $m/z$  28,  $m/z$  12,  $m/z$  29).

A similar effect was observed by Hryha et al. [9]. Taking together the above results, we concluded that the recorded mass loss during sintering contributed to different processes that overlap in this temperature range, i.e. lubricant removal, moisture removal (absorbed by compact constituents), desorption of physically bonded water and start of the reduction of surface iron oxides. The presence of carbon in the investigated composition played an important role as an additional activator of the reduction process in the high temperature range (during the isothermal step). The most relevant reactions that can occur were proposed by Fuentes-Pacheco and Campos [10] and Ciaś et al. [11].

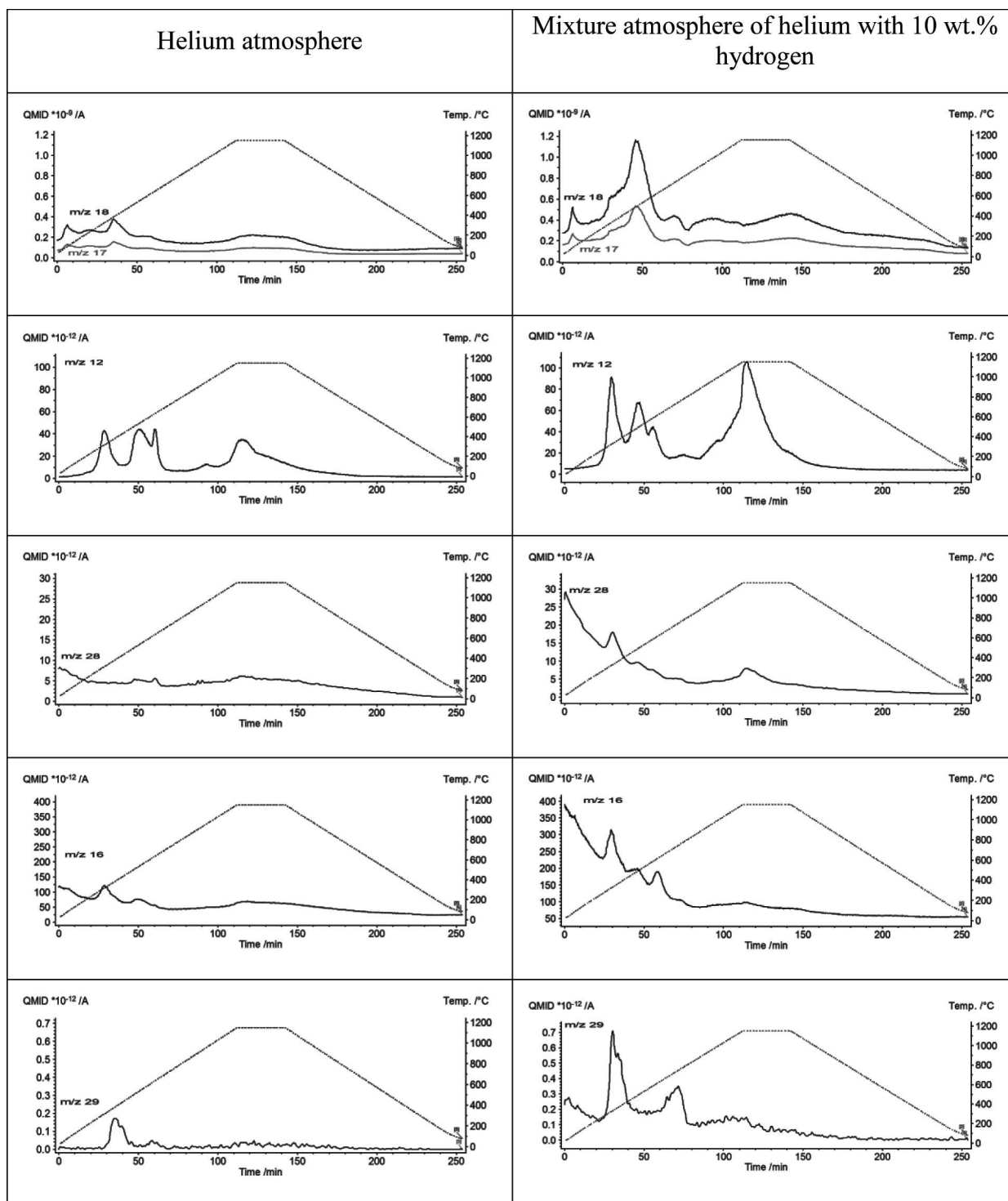


Fig. 12. Mass spectrum (as a QMID mode) of Astaloy CrM with 2 wt.% PCA and 2 wt.% SiC, 2 h milled in the 2:1 ratio, sintered in helium and a mixture of helium with 10 wt.% hydrogen atmosphere

#### 4. Conclusions

The powder to ball mass ratio was an important factor during the mechanical alloying process, which determined fragmentation and work hardening of the mixed powders. The mechanical alloying of Astaloy CrM with the addition of silicon carbide proceeded as a typical

example of the ductile/brittle component system. The presence of silicon slowed down the size reduction.

Compactibility of the milled powder composition was possible with the 2:1 ratio even after 10 h of alloying. When the powder mass to ball mass ratio was 10:1 the alloying products (after 2 h of alloying) were useless for die compaction.

Mechanical alloying played an important role during the sintering process. A dilatometric study indicated strong swelling effects (during heating) which were dependent on the milling time. These phenomena corresponded to the accumulation of compressive strains during milling. Furthermore, the presence of silicon carbide caused the lack of a lattice transformation during heating and cooling.

The mechanical alloying process did not play a significant role in the removal of PCA from the samples.

Registered mass spectrometer data proved that 10 wt.% hydrogen (mixed with helium) is a sufficient amount for the efficient reduction of iron oxides on the powder surfaces. When the silicon carbide was present in the compositions, additional high-temperature reduction (during isothermal sintering) was detected.

#### Acknowledgements

Authors would like to thank the Polish Ministry of Science and Higher Education for support of this work with grant No N N508 393237.

#### REFERENCES

- [1] J.S. Benjamin, *Met. Trans.* **1**, 2943 (1970).
- [2] C. Suryanarayana, *Prog. Mater. Sci.* **1**, 46 (2001).
- [3] R.C. Agarwala, V. Agarwala, J. Karwan-Baczevska, Development of nanograined Ti-Al.-Graphite (Ni-P) by mechanical alloying route, *Archives of Metallurgy and Materials* **53(1)**, 57-61 (2008).
- [4] F.G. Caballero, H.K.D.H. Bhadeshia, K.J.A. Mawella, D.G. Jones, P. Brown, *Material Science and Technology* **17**, 512-516 (2002).
- [5] F.G. Caballero, H.K.D.H. Bhadeshia, K.J.A. Mawella, D.G. Jones, P. Brown, *Material Science and Technology* **18**, 279-282 (2002).
- [6] Sherif El-Eskandarany M. Mechanical Alloying for Fabrication of Advanced Engineering Materials, William Andrew Publishing Norwich, New York, U.S.A. (2001).
- [7] M. Hebdá, Sz. Gądek, J. Kazior, Thermal characteristics and analysis of pyrolysis effects during the mechanical alloying process of Astaloy CrM powders, *Journal of Thermal Analysis and Calorimetry* **108**, 2, 453-460 (2012).
- [8] J.B. Fogagnolo, F. Velasco, M.H. Robert, J.M. Torralba, *Materials Science and Engineering* **A342**, 131-143 (2003).
- [9] E. Hryha, L. Cajkova, E. Dudrova, L. Nyborg, Euro PM2008 – Proceedings, Sintered Steels 109-114 (2008).
- [10] L. Fuentes-Pacheco, M. Campos, *Powder Metall.* **46**, 165 (2003).
- [11] A. Ciałś, S.C. Mitchell, K. Pilch, H. Ciałś, M. Sułowski, A.S. Wroński, *Powder Metall.* **46**, 165 (2003).